

Optimization of the Compensation Capacitors for Megahertz Wireless Power Transfer Systems

Zefan Tang, Minfan Fu, Ming Liu, Chengbin Ma*

University of Michigan - Shanghai Jiao Tong University Joint Institute Shanghai, China
zftang@sjtu.edu.cn, fuminfan@sjtu.edu.cn, mikeliu@sjtu.edu.cn, chbma@sjtu.edu.cn

Abstract—A wireless power transfer system can increase its system frequency to several Megahertz for large spatial freedom. A MHz system usually uses the same compensation as those kHz systems. Traditionally, the rectifier is modeled as a pure resistive load for the coupling coils when designing the compensation capacitors. However, the rectifier input reactance cannot be ignored for MHz systems. This reactance can affect the system resonance and is usually not considered when designing the compensation capacitors. This paper analyzes the rectifier input impedance and discusses its undesirable effects. A non-zero phase is shown to exist seeing into the coupling coils for MHz WPT system. In order to limit the phase, the optimal compensation capacitors are discussed and found. Finally, a 6.78 MHz system is used to verify the proposed optimal compensation method. It shows the phase variation can be limited from the original range $[15^\circ - 35^\circ]$ to the optimal range $[-5^\circ - 5^\circ]$.

Index Terms—Wireless power transfer, compensation, high-frequency rectifier, input reactance, phase

I. INTRODUCTION

Recently, resonance inductive coupling becomes a promising wireless power transfer (WPT) technology. Its unique advantages make WPT-based charging methods challenge the traditional wire-connected charging methods in different areas, such as wearable devices, mobile phones, household appliances, and even high-power electric vehicles [1]–[5]. For the aforementioned applications, different WPT solutions should be designed according to the specific requirements, such as power level, transfer distance, radiation limit and system reliability. For those small or medium power (< 40 Watt) devices, it is preferred to increase the resonance frequency to several Megahertz for large spacial freedom [6], [7].

Similar to kHz WPT systems, a MHz system consists of all the necessary power conversion blocks, including a power amplifier for dc/ac conversion, the coupling coils for ac/ac conversion, and a rectifier for ac/dc conversion [8]–[10]. In such a system, each function block can be analyzed individually or optimized in a whole system. For example, [11] demonstrates high-efficiency or tunable power amplifiers; [12]–[15] give the fundamental circuit analysis for the coupling coils; [9] focuses on the whole system efficiency analysis, and [8], [10] carry out a system-level optimal load tracking. Among these contributions, the most fundamental work for WPT systems is to design the compensation methods for the coupling coils. A properly designed compensation method can significantly enhance the power transfer capability among the coupling coils and provide a resistive load for

the ac source. Many published works have well solved this issue. Among these works, four basic compensation solutions have been widely used and accepted, including series-series (SS), series-parallel (SP), parallel-series (PS), and parallel-parallel (PP) [16]. Also some high order compensations can be found in some systems [14], [15], [17]–[20]. However, the load of the coupling coils, i.e., the rectifier input impedance, are modeled as a pure resistor for most papers above. This simple assumption is no longer valid for a rectifier working at several MHz. Such a rectifier is shown to have non-zero input reactance [8], [10]. This input reactance would make the system deviate from the original design and even affect the transfer characteristics of the coils. Therefore, it is necessary to analyze the influence of the rectifier input reactance and give corresponding compensation solutions.

Theoretically, the problems caused by the rectifier input reactance can be solved by the auto-tuning mechanism, such as the tuning of impedance matching circuits or coupling coils's positions [21]. However, it requires reliable detection circuits and smart control mechanisms. Besides, the use of more circuit components will increase the system cost and complexity. In a system, it is more attractive to use fixed capacitors for compensation. Such a system is proposed to work in an environment with various uncertainties, including the coils distance and final load variation. Generally, the SS compensation is the most attractive solution because its compensation capacitors are independent of the final load and the coupling condition [8], [16]. However, as mentioned above, this independence is no longer valid due to the rectifier input reactance. Therefore, this paper aims at finding optimal SS compensation capacitors to accommodate the high-frequency system, especially considering the actual rectifier influence.

This paper will first review the traditional compensation method. Then a simulation-based analysis is carried out to show the characteristics of the rectifier input reactance and its associated influence for the coupling coils. In order to minimize the rectifier input reactance effects, the rectifier is modeled as a non-pure-resistive load for the coupling coils. In such a circuit model, different combinations of SS compactors are evaluated in simulation to show their influence. Then optimal compensation capacitors are found through a global search and shown to be valid in simulation. In the final experiment, it shows that the use of optimal compensation capacitors can greatly minimize the effects caused by the rectifier input reactance for a 6.78 MHz system.

II. SYSTEM ANALYSIS

A. Traditional Compensation

Fig. 1 shows the circuit model for series-series (SS) compensated WPT system. L_1, L_2, R_1, R_2 are the self-inductances and self-resistances of the coils. M_{12} is the mutual inductance between the transmitting coil and receiving coil. The traditional SS compensation method is to use C_1 and C_2 to form resonance circuit by

$$j\omega L_i + \frac{1}{j\omega C_i} = 0, \quad i = 1 \text{ or } 2, \quad (1)$$

where ω is the resonance frequency.

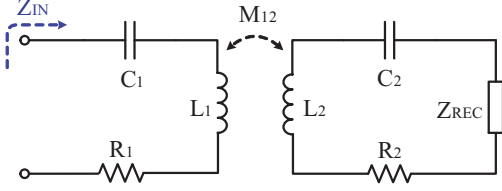


Fig. 1. The circuit model for series-series compensation coils.

B. Rectifier Input Reactance

With the traditional compensation, the input impedance of coupling coils (Z_{IN}) can be expressed by

$$Z_{IN} = \frac{\omega^2 M_{12}^2}{R_2 + Z_{REC}} + R_1, \quad (2)$$

where Z_{REC} is the direct load of the receiving coil. Usually, a rectifier is connected to the receiving coils and its input impedance is just Z_{REC} . The resonance condition (1) is derived based on the assumption that Z_{REC} is pure resistive. And a pure resistive Z_{REC} can ensure a pure resistive Z_{IN} [refer to (2)]. However, this assumption for resistive Z_{REC} is no longer valid for high-frequency system. Fig. 2 gives the circuit model for a full-bridge rectifier. At high frequency, the device parasitic parameters become obvious and make the diode no longer an ideal switch. These undesirable parameters will introduce ineligious imaginary part for Z_{REC} , i.e., input reactance. Therefore, the rectifier input impedance should be modeled as

$$Z_{REC} = R_{REC} + jX_{REC}, \quad (3)$$

where R_{REC} is the input resistance and X_{REC} is the input reactance.

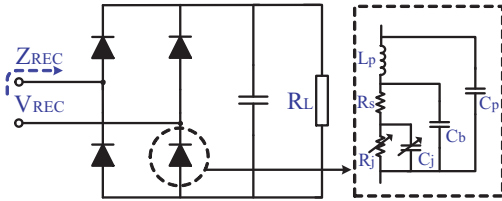


Fig. 2. Full-bridge rectifier topology and high-frequency diode circuit model.

In order to accurately capture Z_{REC} , a circuit-model-based simulation is carried out in a widely-used RF software

Advanced Design System (ADS), provided by Keysight Technologies Inc.. The rectifier is first analyzed individually with the diode spice model (DFLS406L from Diodes Inc. and used in the final experimental system). During the simulation, the rectifier input voltage V_{REC} is fixed at 20 V and the load resistance R_L is varied from 10 Ω to 100 Ω . Fig. 3 gives the rectifier input resistance and reactance for different frequencies. At low frequency (power electronics band), R_{REC} is almost linearly proportional to R_L , and X_{REC} is negligible compared to R_{REC} . At high frequency (RF band), the trend of R_{REC} experiences small variation, but X_{REC} becomes obvious and compatible to the R_{REC} . These results can be well explained by the diode model given in Fig. 2. At high frequency, those shunt capacitors (C_j, C_b and C_p in Fig. 2) will become significant and introduce capacitance for Z_{REC} , i.e., the negative X_{REC} in Fig. 3.

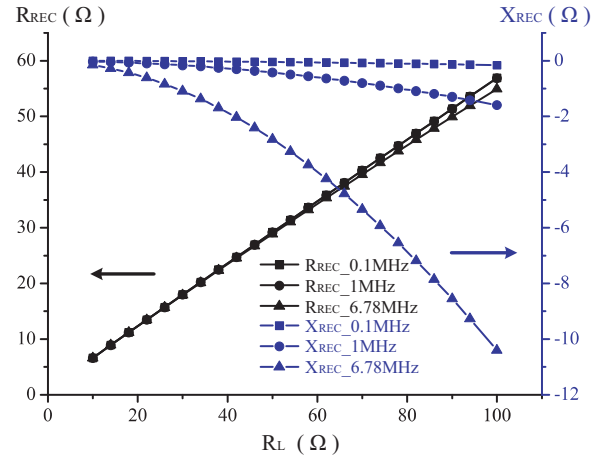


Fig. 3. Rectifier input resistance R_{REC} and input reactance X_{REC} for different frequencies.

C. The Influence of Z_{REC}

The input impedance of coupling coils Z_{IN} can be expressed by substituting (3) into (2) as follows,

$$Z_{IN} = \frac{\omega^2 M_{12}^2}{R_2 + R_{REC} + jX_{REC}} + R_1. \quad (4)$$

The resistance and reactance of Z_{IN} can be derived as

$$R_{IN} = \frac{\omega^2 M_{12}^2 (R_2 + R_{REC})}{(R_2 + R_{REC})^2 + X_{REC}^2} + R_1, \quad (5)$$

and

$$X_{IN} = \frac{-\omega^2 M_{12}^2 X_{REC}}{(R_2 + R_{REC})^2 + X_{REC}^2}. \quad (6)$$

The phase of Z_{IN} is defined as

$$\theta = \tan^{-1}\left(\frac{X_{IN}}{R_{IN}}\right). \quad (7)$$

Due to the complicated characteristics of the diodes, it is impractical to describe the rectifier input impedance (R_{REC} and X_{REC}) in accurately mathematical expressions of R_L . In order to evaluate the influence of Z_{REC} , a simulation of

the system including both the coupling coils and the rectifier in ADS is better to be carried out. The coils' parameters are given in Table I for a 6.78 MHz system. And the compensation capacitors are chosen according to (1). In such a system, a 6.78 MHz constant current source is used to drive the transmitting coil. The current RMS value is set at 0.5 A. Fig. 4 gives Z_{IN} for different R_L . According to (2), R_{IN} is reversely proportional to R_L as shown in Fig. 4. The negative X_{REC} will cause an inductive component for Z_{IN} , i.e., the positive X_{IN} . In this WPT system, the phase of Z_{IN} is also given in Fig. 4, and it increases with R_L . In applications, such a large phase variation is undesirable for the power amplifier. Therefore, it is meaningful to modify the traditional compensation method to accommodate the high-frequency system.

TABLE I
COILS PARAMETERS

Parameters	Value
Inductance (L_1, L_2)	3.34 μH
Resistance (R_1, R_2)	0.8 Ω
Mutual inductance (M_{12})	0.55 μH

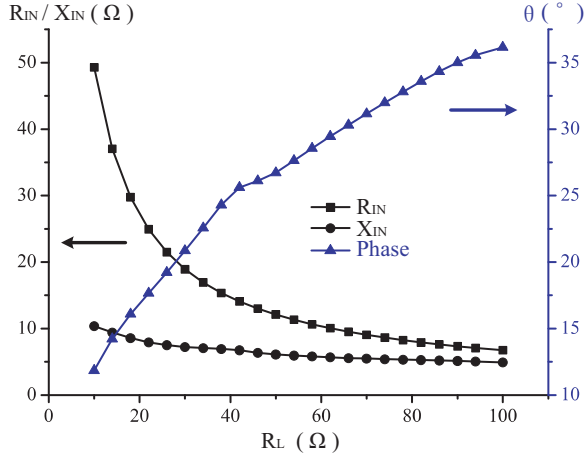


Fig. 4. The input impedance Z_{IN} and its phase for different R_L at 6.78 MHz.

III. OPTIMAL COMPENSATION CAPACITORS

A. The Influence of Compensation Capacitors

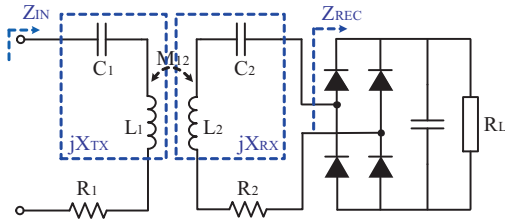


Fig. 5. System configuration

Usually, impedance matching networks are used to eliminate the undesirable θ . However, these additional circuits will

inevitably introduce component loss. This paper is proposed to optimize the SS compensation capacitors for a high-frequency WPT system. The circuit model is shown in Fig. 5. The value of compensation capacitors should be properly designed instead of calculated through (1). For convenience, the coil inductance and compensation capacitance can be combined and represented by their net reactance at the transmitting side and receiving side respectively [jX_{TX} and jX_{RX} in Fig. 5]. Thus, it has

$$\begin{cases} X_{TX} = \omega L_1 - \frac{1}{\omega C_1} \\ X_{RX} = \omega L_2 - \frac{1}{\omega C_2} \end{cases} \quad (8)$$

Then (1) is equivalent to

$$\begin{cases} X_{TX} = 0 \\ X_{RX} = 0 \end{cases} \quad (9)$$

Considering the rectifier input reactance, the input impedance of coupling coils is expressed as

$$Z_{IN} = \frac{\omega^2 M_{12}^2}{R_2 + R_{REC} + jX_{RX} + jX_{REC}} + R_1 + jX_{TX}. \quad (10)$$

The resistance and reactance of Z_{IN} can be represented as follows,

$$R_{IN} = \frac{\omega^2 M_{12}^2 (R_2 + R_{REC})}{(R_2 + R_{REC})^2 + (X_{RX} + X_{REC})^2} + R_1, \quad (11)$$

and

$$X_{IN} = \frac{\omega^2 M_{12}^2 (-X_{RX} - X_{REC})}{(R_2 + R_{REC})^2 + (X_{RX} + X_{REC})^2} + X_{TX}. \quad (12)$$

Here, the study of compensation capacitors' effects are achieved by evaluating the effects of different X_{TX} and X_{RX} [refer to (8)], since the coils inductors are fixed. According to (11) and (12), X_{RX} affects both R_{IN} and X_{IN} and X_{TX} only affects X_{IN} . In order to reduce X_{IN} , the optimal X_{TX} is supposed to be negative due to the original positive X_{IN} [refer to (12) and Fig. 4]. Similarly, the optimal X_{RX} is supposed to be positive due to the existence of negative X_{REC} [refer to Fig. 3].

In simulation, the influence of different X_{TX} and X_{RX} are evaluated individually and compared with the traditional compensation method, i.e., $X_{TX} = X_{RX} = 0 \Omega$. Fig. 6, Fig. 7 and Fig. 8 give R_{IN} , X_{IN} and θ for different X_{TX} and X_{RX} , respectively. In Fig. 6, it shows different X_{RX} have limited effects on R_{IN} . Note that X_{TX} does not affect R_{IN} [refer to (11)]. Compared to the limited effects on R_{IN} , X_{IN} and θ can be significantly affected by different X_{TX} and X_{RX} as shown in Fig. 7 and Fig. 8. When R_L is small, the use of positive X_{RX} can reduce X_{IN} and keep θ near the zero-phase point. But its influence can be ignored for large R_L . Compare to X_{RX} , the influence of X_{TX} is more obvious for large R_L . Therefore, it is reasonable to find an optimal pair of compensation capacitors to achieve small θ for a large R_L range.

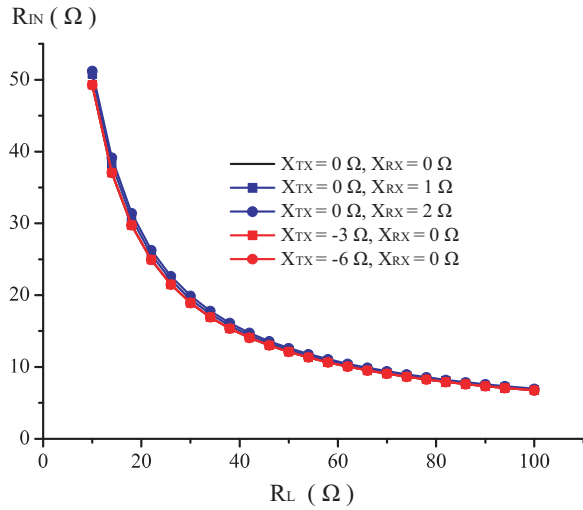


Fig. 6. The input resistance R_{IN} for different X_{TX} and X_{RX} .

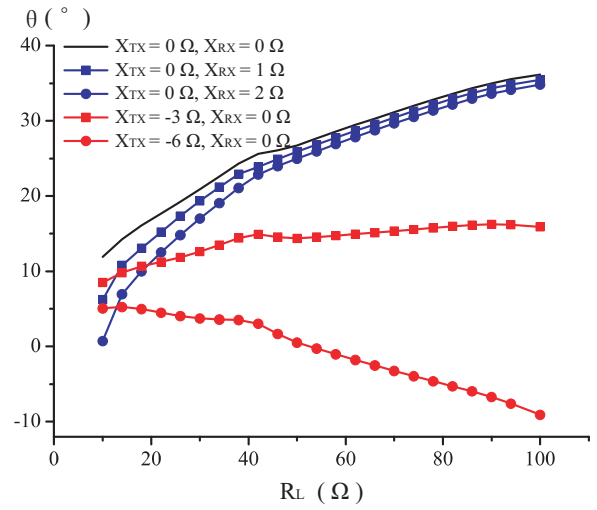


Fig. 8. The phase of Z_{IN} θ for different X_{TX} and X_{RX} .

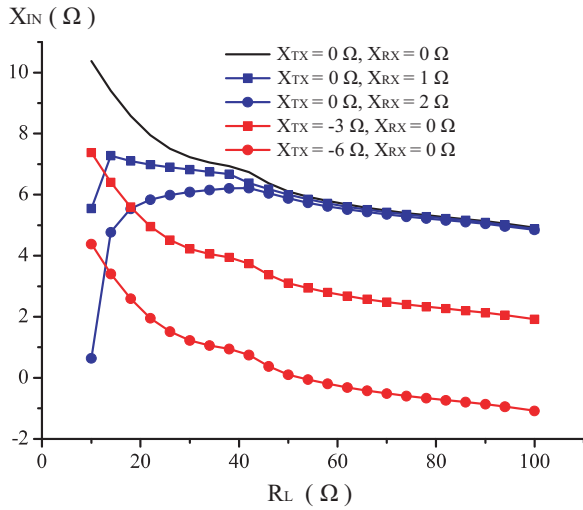


Fig. 7. The input reactance X_{IN} for different X_{TX} and X_{RX} .

model is known. However, it is difficult to describe the high-frequency switching behavior, especially obtaining its input reactance X_{REC} . Without X_{REC} , the optimal X_{TX} and X_{RX} can not be directly derived. In this paper, a global search is carried out in ADS to obtain the optimal X_{TX} and X_{RX} . The parameters here are the same as those in Section II-B. The step for X_{TX} and X_{RX} is 0.01Ω . The optimal X_{TX} and X_{RX} are -5.88Ω and 1.15Ω , respectively.

Fig. 9 and Fig. 10 show the comparison of traditional compensation and the optimal compensation. The comparison for Z_{IN} is shown in Fig. 9. With the optimal compensation, X_{IN} can be significantly reduced, and R_{IN} almost doesn't change. The phase comparison is shown in Fig. 10. Compared with traditional compensation, the proposed optimal compensation can limit the variation of θ in a small range, i.e., -5° to 5° .

B. Parameters Optimization

Section III-A shows X_{TX} and X_{RX} have different effects on Z_{IN} and θ . Therefore, it is promising to combine the advantages of X_{TX} and X_{RX} for different R_L , namely, X_{RX} for small R_L and X_{TX} for large R_L . It is proposed that the combination of optimal X_{TX} and X_{RX} can limit θ variation within a small range. The static optimization problem can be stated:

- Objective: Minimize the peak θ in a R_L range.
- Constrains: The system can be described by the model of the coupling coils [refer to (11)-(12)] and the rectifier [refer to Fig.3].
- Control variables: X_{TX} and X_{RX} , i.e., the compensation capacitors C_1 and C_2 .

Usually, the traditional parameters optimization method can be directly applied if the rectifier impedance transformation

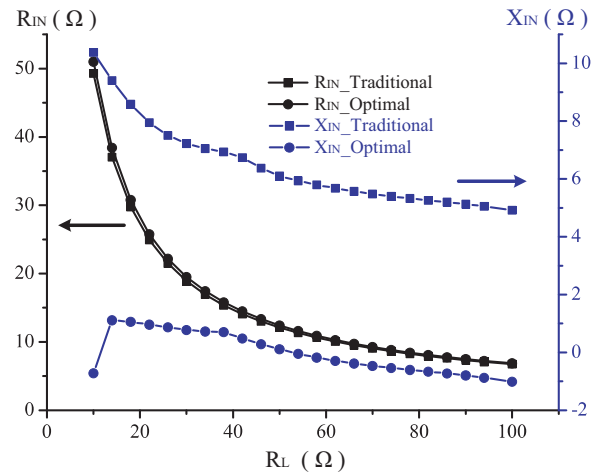


Fig. 9. Comparison for Z_{IN} in simulation.

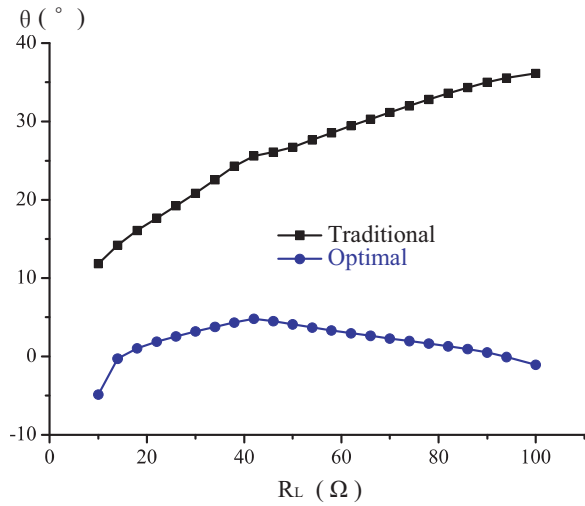


Fig. 10. Comparison for θ in simulation.

C. System Efficiency

In a WPT system as shown in Fig. 5, the system efficiency η_{SYS} (from the transmitting coil to the load R_L) can be calculated as (13) shows.

According to (13), η_{SYS} can be affected by the value of X_{RX} . A small value of $(X_{RX} + X_{REC})^2$ leads to a bigger η_{SYS} . In 6.78 MHz WPT system, since X_{REC} is negative (as shown in Fig. 3), a small positive value of X_{RX} in the optimal compensation will make $(X_{RX} + X_{REC})^2$ smaller. Therefore, with the optimal compensation method η_{SYS} will become a little larger, which is verified in the simulation in Fig. 11.

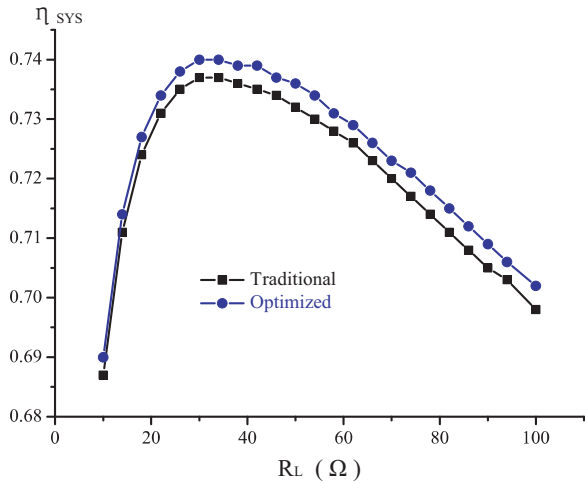


Fig. 11. Comparison for η_{SYS} in simulation.

IV. EXPERIMENTAL VERIFICATION

The system setup for the final experiment is shown in Fig. 12. This measurement platform consists of a 6.78 MHz power amplifier, two coupling coils, a full-bridge rectifier and an electronic load. In the experiment, the power amplifier can be tuned to provide a constant input current to drive the system for different R_L . The RMS value of this current is set at 0.5A.

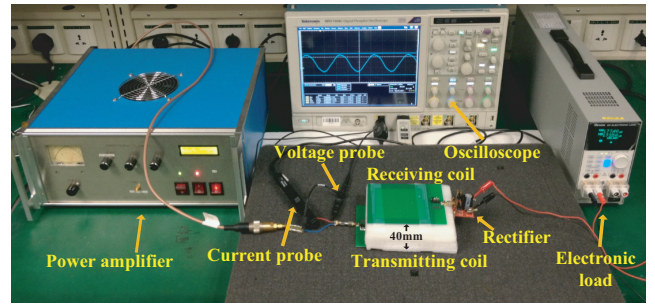


Fig. 12. Experiment setup.

The parameters for the coupling coils and rectifier are the same as that used in the simulation. Through the current and voltage probes, the measured waveforms can be used to obtain Z_{IN} and its phase with an inverse FFT calculation. Before the experiment, a pure 50 Ω RF load is used for calibration and the initial phase difference between probes can be eliminated.

Fig. 13 shows the input impedance Z_{IN} seeing into the coupling coils. Using the optimal compensation, the input reactance X_{IN} can be significantly reduced to a very low level (-1 Ω to 2 Ω). And the input resistance R_{IN} has little variation. The phase comparison is given in Fig. 14. Using the traditional compensation, the phase variation is from 15 $^\circ$ to 35 $^\circ$. When the optimal compensation is applied, the original large phase variation can be successfully reduced to a level from -5 $^\circ$ to 5 $^\circ$. Fig. 15 gives the efficiency comparison. It shows that with the optimal compensation method the system efficiency will be improved in a certain degree. Compared to the traditional compensation, the optimal compensation shows its advantages in limiting the phase change and improving the system efficiency. These experiment results are well consistent with the simulation results given in Fig. 9, Fig. 10 and Fig. 11.

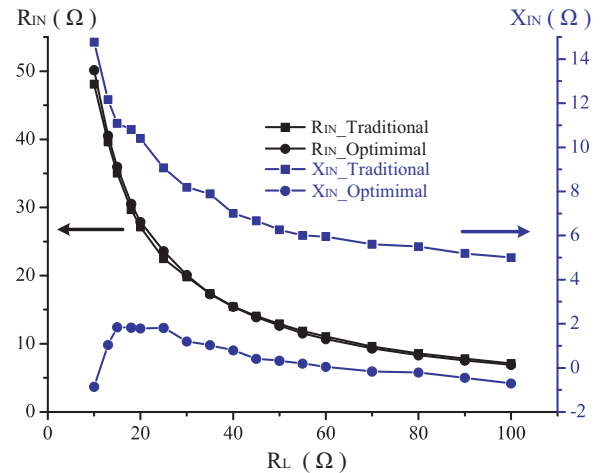


Fig. 13. Comparison for Z_{IN} in experiment.

V. CONCLUSION

In this paper, the input impedance seen from the rectifier is first analyzed in ADS simulation. The occurrence of reactance

$$\eta_{SYS} = \frac{\omega^2 M_{12}^2 R_L}{\omega^2 M_{12}^2 (R_2 + R_{REC}) + R_1 (R_2 + R_{REC})^2 + R_1 (X_{RX} + X_{REC})^2} \quad (13)$$

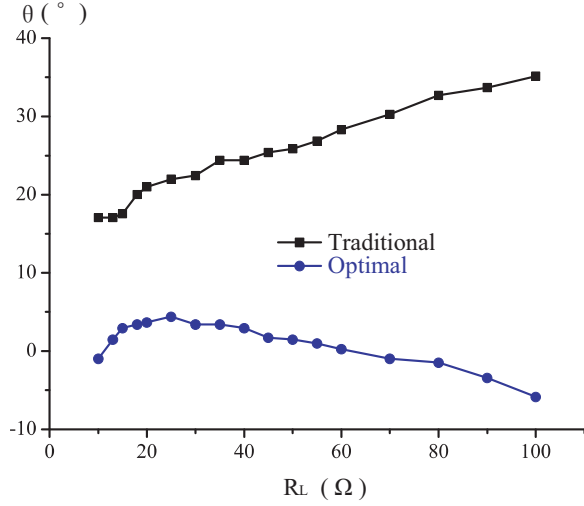


Fig. 14. Comparison for θ in experiment.

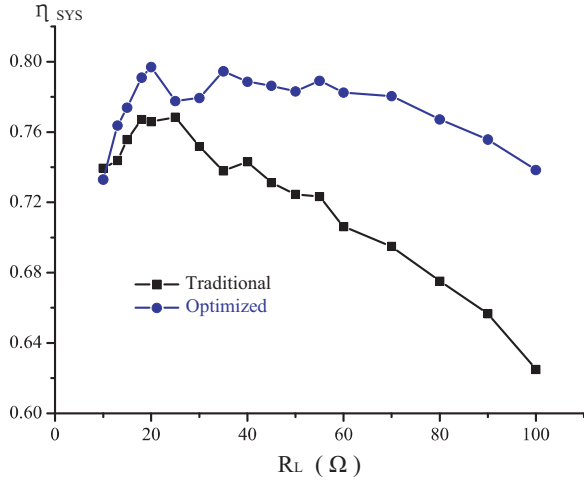


Fig. 15. Comparison for η_{SYS} in experiment.

is shown to introduce a large phase for the input impedance of a traditional SS compensation coupling coils. Based on the characteristics of high-frequency rectifier, a circuit model is built and analyzed in simulation when considering the rectifier input reactance. An optimal pair of SS compensation capacitors is found to limit the phase variation. Finally, a 6.78 MHz system is implemented in experiment. It shows that the optimal compensation capacitors can minimize the peak phase for the input impedance of the coils successfully.

REFERENCES

[1] P. Li and R. Bashirullah, "A wireless power interface for rechargeable battery operated medical implants," *IEEE Trans. Circuits Syst. II, Exp. Briefs*, vol. 54, no. 10, pp. 912–916, 2007.

[2] A. P. Hu, *Wireless/Contactless Power Supply:-Inductively coupled resonant converter solutions*. Saarbrücken, Germany: VDM Publishing, 2009.

[3] C.-S. Wang, O. H. Stielau, and G. A. Covic, "Design considerations for a contactless electric vehicle battery charger," *IEEE Trans. Ind. Electron.*, vol. 52, no. 5, pp. 1308–1314, 2005.

[4] N. A. Keeling, G. A. Covic, and J. T. Boys, "A unity-power-factor IPT pickup for high-power applications," *IEEE Trans. Ind. Electron.*, vol. 57, no. 2, pp. 744–751, 2010.

[5] W. Zhong, X. Liu, and S. R. Hui, "A novel single-layer winding array and receiver coil structure for contactless battery charging systems with free-positioning and localized charging features," *IEEE Trans. Ind. Electron.*, vol. 58, no. 9, pp. 4136–4144, 2011.

[6] J. J. Casanova, Z. N. Low, and J. Lin, "A loosely coupled planar wireless power system for multiple receivers," *IEEE Trans. Ind. Electron.*, vol. 56, no. 8, pp. 3060–3068, 2009.

[7] D. Ahn and S. Hong, "Effect of coupling between multiple transmitters or multiple receivers on wireless power transfer," *IEEE Trans. Ind. Electron.*, vol. 60, no. 7, pp. 2602–2613, 2013.

[8] M. Fu, C. Ma, and X. Zhu, "A cascaded boost-buck converter for high efficiency wireless power transfer systems," *IEEE Trans. Ind. Informat.*, vol. 10, no. 3, pp. 1972–1980, 2014.

[9] D. Krschner and C. Rathge, "Maximizing dc-to-load efficiency for inductive power transfer," *IEEE Trans. Power Electron.*, vol. 28, no. 5, pp. 2437–2447, 2013.

[10] M. Fu, H. Yin, X. Zhu, and C. Ma, "Analysis and tracking of optimal load in wireless power transfer systems," *IEEE Trans. Power Electron.*, vol. 30, no. 7, pp. 3952–3963, 2015.

[11] S. Aldhafer, P. C. Luk, and J. F. Whidborne, "Tuning class e inverters applied in inductive links using saturable reactors," *IEEE Trans. Power Electron.*, vol. 29, no. 6, pp. 2969–2978, 2014.

[12] C.-S. Wang, O. H. Stielau, and G. A. Covic, "Load models and their application in the design of loosely coupled inductive power transfer systems," in *Power System Technology, 2000. Proceedings. PowerCon 2000. International Conference on*, vol. 2. IEEE, 2000, pp. 1053–1058.

[13] M. Fu, T. Zhang, C. Ma, and X. Zhu, "Efficiency and optimal loads analysis for multiple-receiver wireless power transfer systems," *IEEE Trans. Microw. Theory Tech.*, vol. 63, no. 3, pp. 801–812, 2015.

[14] S. Cheon, Y. Kim, S. Kang, M. Lee, J. Lee, and T. Zyung, "Circuit-model-based analysis of a wireless energy-transfer system via coupled magnetic resonances," *IEEE Trans. Ind. Electron.*, vol. 58, no. 7, pp. 2906–2914, 2011.

[15] L. Chen, S. Liu, Y. C. Zhou, and T. J. Cui, "An optimizable circuit structure for high-efficiency wireless power transfer," *IEEE Trans. Ind. Electron.*, vol. 60, no. 1, pp. 339–349, 2013.

[16] C. Wang, G. A. Covic, and O. H. Stielau, "Power transfer capability and bifurcation phenomena of loosely coupled inductive power transfer systems," *IEEE Trans. Ind. Electron.*, vol. 51, no. 1, pp. 148–157, 2004.

[17] C.-Y. Huang, J. T. Boys, and G. A. Covic, "Lcl pickup circulating current controller for inductive power transfer systems," *IEEE Trans. Power Electron.*, vol. 28, no. 4, pp. 2081–2093, 2013.

[18] Z. Pantic, S. Bai, and S. Lukic, "Zcs-compensated resonant inverter for inductive-power-transfer application," *IEEE Trans. Ind. Electron.*, vol. 58, no. 8, pp. 3500–3510, 2011.

[19] C.-S. Wang, G. A. Covic, and O. H. Stielau, "Investigating an lcl load resonant inverter for inductive power transfer applications," *IEEE Trans. Power Electron.*, vol. 19, no. 4, pp. 995–1002, 2004.

[20] A. P. Sample, D. A. Meyer, J. R. Smith *et al.*, "Analysis, experimental results, and range adaptation of magnetically coupled resonators for wireless power transfer," *IEEE Trans. Ind. Electron.*, vol. 58, no. 2, pp. 544–554, 2011.

[21] T. C. Beh, M. Kato, T. Imura, S. Oh, and Y. Hori, "Automated impedance matching system for robust wireless power transfer via magnetic resonance coupling," *IEEE Trans. Ind. Electron.*, vol. 60, no. 9, pp. 3689–3698, 2013.